

Enhanced terahertz emission from a multilayered low temperature grown GaAs structure

Samir Rihani, Richard Faulks, Harvey E. Beere, Ian Farrer, Michael Evans, David A. Ritchie, and Michael Pepper

Citation: [Applied Physics Letters](#) **96**, 091101 (2010); doi: 10.1063/1.3332587

View online: <http://dx.doi.org/10.1063/1.3332587>

View Table of Contents: <http://scitation.aip.org/content/aip/journal/apl/96/9?ver=pdfcov>

Published by the [AIP Publishing](#)

Articles you may be interested in

[64 \$\mu\$ W pulsed terahertz emission from growth optimized InGaAs/InAlAs heterostructures with separated photoconductive and trapping regions](#)

Appl. Phys. Lett. **103**, 061103 (2013); 10.1063/1.4817797

[Terahertz-frequency photoconductive detectors fabricated from metal-organic chemical vapor deposition-grown Fe-doped InGaAs](#)

Appl. Phys. Lett. **98**, 121107 (2011); 10.1063/1.3571289

[Improved sensitivity of terahertz detection by GaAs photoconductive antennas excited at 1560 nm](#)

Appl. Phys. Lett. **97**, 201110 (2010); 10.1063/1.3519480

[Terahertz wave emission and detection using photoconductive antennas made on low-temperature-grown InGaAs with 1.56 \$\mu\$ m pulse excitation](#)

Appl. Phys. Lett. **91**, 011102 (2007); 10.1063/1.2754370

[Systematic pump-probe terahertz wave emission spectroscopy of a photoconductive antenna fabricated on low-temperature grown GaAs](#)

J. Appl. Phys. **96**, 3635 (2004); 10.1063/1.1786667

A promotional banner for Applied Physics Reviews. On the left is a small image of the journal cover for 'Applied Physics Reviews', which shows a diagram of a device structure. The main part of the banner has a blue background with a glowing light effect. The text 'NEW Special Topic Sections' is prominently displayed in white. Below this, on an orange background, it says 'NOW ONLINE' in yellow, followed by 'Lithium Niobate Properties and Applications: Reviews of Emerging Trends' in white. The AIP Applied Physics Reviews logo is in the bottom right corner.

NEW Special Topic Sections

NOW ONLINE
Lithium Niobate Properties and Applications:
Reviews of Emerging Trends

AIP Applied Physics Reviews

Enhanced terahertz emission from a multilayered low temperature grown GaAs structure

Samir Rihani,^{1,a)} Richard Faulks,¹ Harvey E. Beere,¹ Ian Farrer,¹ Michael Evans,² David A. Ritchie,¹ and Michael Pepper^{1,2,b)}

¹*Cavendish Laboratory, University of Cambridge, Cambridge CB3 0HE, United Kingdom*

²*TeraView Ltd., Cambridge CB4 0WS, United Kingdom*

(Received 2 December 2009; accepted 3 February 2010; published online 1 March 2010)

We report the use of a multilayered structure comprising of alternating layers of low temperature grown GaAs and high temperature grown AlAs, as a terahertz (THz) photoconductive antenna emitter and receiver. Devices based on $10 \times 10 \mu\text{m}^2$ mesa defined photoconductive gaps were fabricated on the multilayered structure, and a comparison made to conventional planar devices. The mesa defined photoconductive antennas allowed successive contact through the multilayered structure, which resulted in an increase in THz emission power and detection responsivity with increasing number of layers in contact with the antenna electrodes. A comparison with a conventional single layered device, processed in an identical mesa geometry, confirmed that the enhancement in THz emission is solely due to the multilayered nature of the device, whereas the improved receiver performance can be partially attributed to the mesa geometry. © 2010 American Institute of Physics. [doi:10.1063/1.3332587]

Terahertz generation using photoconductive switches is an attractive technique which has led to the development and commercial exploitation of terahertz (THz) technology.¹ The main attractions to this technology are room temperature operation and the simple nature of the device, which mainly involves the deposition of two metal electrodes on top of an ultrafast carrier material, such as low temperature grown GaAs (LT-GaAs).

To date, LT-GaAs remains the material of choice for broad band THz generation and detection due to its high resistivity and short carrier lifetime. So far, most studies have concentrated on improving the material qualities of LT-GaAs to enhance THz emission and detection. However, since the key physical properties of LT-GaAs are determined by the growth temperature and postgrowth anneal,² there is limited scope of development once the carrier lifetime and resistivity of the material has been optimized. There have been many attempts to improve the antenna designs which play a significant role in the THz efficiency and output powers.³ Another approach is the use of AlAs/GaAs Bragg reflectors to enhance the optical absorption of the photomixer.^{4,5} An alternative design incorporates a traveling wave design to circumvent the RC time constant of the device, resulting in an increase in the THz output power.⁶ Recently Mikulics *et al.*⁷ reported up to 100% increase in the THz output power from LT-GaAs photomixers by using recessed contacts instead of conventional surface contacts.

Most of the above approaches have relied on a conventional $1 \mu\text{m}$ LT-GaAs active region device structure. In this work, we report the use of a multilayered structure composed of alternating layers of LT-GaAs and high temperature AlAs (HT-AlAs), as a THz emitter and receiver. Devices based on $10 \times 10 \mu\text{m}^2$ mesa defined photoconductive gaps were fabricated using the multilayered structure, which consisted of

$4 \times 250 \text{ nm}$ LT-GaAs layers separated by 33 nm HT-AlAs isolation layers; this mimics the thickness of the active layer in a standard conventional " $1 \mu\text{m}$ LT-GaAs" photoconductive switch. The mesa geometry allowed contacts to be made independently to successive LT-GaAs layers, M1 had contact to only the top LT-GaAs layer, M2 had contacts to the top two LT-GaAs layers, etc. A schematic diagram of the planar geometry and each mesa type device, fabricated on both the multilayer and a conventional " $1 \mu\text{m}$ " single layer LT-GaAs structure, is shown in Fig. 1(a). The entire active region is isolated from the semi-insulating GaAs (SI-GaAs) substrate by a 100 nm thick AlAs layer. The samples were grown nominally at a temperature of 240°C , except for the AlAs layers which were grown at 500°C . This has been shown not to significantly anneal the underlying LT-GaAs layers in the multilayered structure.⁸ As per our standard process, the material was annealed *ex situ* at 500°C for 10 min to optimize the performance.²

Using standard photolithography, a $2 \mu\text{m}$ gap bow tie antenna was fabricated on top of each sample. For the planar structures, including both the conventional single layer (C-Planar) and the multilayered (M-Planar), only Ti/Au antenna was evaporated on the surface of the material. For the mesa type devices, a $10 \times 10 \mu\text{m}^2$ mesa was first etched down to

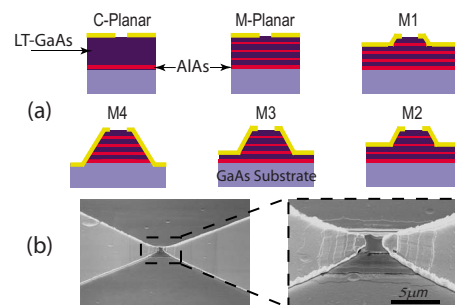


FIG. 1. (Color online) (a) A schematic diagram of the sample set used for the experiment. (b) An Electron microscope image of the M4 mesa device fabricated on the multilayer LT-GaAs structure.

^{a)}Electronic addresses: sr444@cam.ac.uk and s.rihani@gmail.com.

^{b)}Present address: Department of Electronic and Electrical Engineering, University College, London WC1E 6BT.

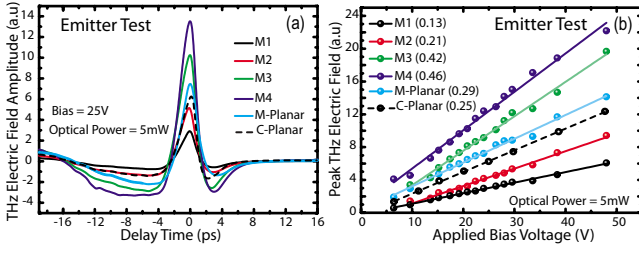


FIG. 2. (Color online) (a) THz time domain signal from both, planar and mesa defined photoconductive switches. (b) Bias dependence of the emitted THz radiation, numbers between brackets indicate the slope of the linear fit.

the desired depth, and then the Ti/Au bow tie antenna was thermally evaporated. Figure 1(b) is a scanning electron microscope (SEM) image of the M4 device where the etch was through the entire multilayered structure reaching the SI-GaAs substrate. The individual LT-GaAs/HT-AlAs layers can be clearly seen in the SEM image. We also observe that the lateral etching in this multilayered structure was much faster than the vertical etching, which resulted in significant sloped side walls for the etched mesa. Although this was useful in obtaining robust side contacts, it did lead to increasing the effective gap sizes for the underlying LT-GaAs layers. The devices were tested using a standard photoconductive sampling setup.⁹ The terahertz pulses were collected from each device as a function of optical power and bias voltage. In the emitter (receiver) test a reference LT-GaAs photoconductive device is used as a receiver (emitter) under a constant optical excitation of 5 mW.

Figure 2(a) shows the terahertz time domain signal from all the emitter devices (both planar and mesa) fabricated on the multilayered structure. Clearly the output THz electric field increases with increasing number of layers in contact with the antenna electrodes, suggesting a contribution from each layer to the THz generation process. The results of Fig. 2(a) show that, under 5 mW of optical power and 25 V bias voltage, the mesa multilayered device M4, is up to four times and 20 times more power efficient than the planar device (M-Planar) and the M1 mesa device, respectively ($P_{\text{THz}} \propto E_{\text{THz}}^2$). This order of magnitude increase in the emitted THz power indicates the potential of this type of device structure as an efficient THz emitter. Note that the performance of both planar devices (M-Planar and C-Planar) were approximately equivalent.

The THz peak bias dependence, Fig. 2(b), shows a linear behavior in all the devices across the entire bias range. Furthermore, the calculated slopes, of the linear fits, show an increase with increasing contacted layers. This is strong evidence that the enhanced THz emission, observed in Fig. 2, is related to the contribution of the extra contacted layers. In addition, we note the similar slopes for both types of planar devices used. At this stage it is not clear why the enhanced THz emission, over planar structures, is only seen for more than two contacted layers. Possible factors, affecting the performance of the M1 and M2 devices, could be related to variation of gap size with mesa depth and changes in the capacitance and resistance of the device due to the larger volume of the addressed active region in these mesa type devices.

Figure 3(a) shows the emitted peak THz electric field amplitude as a function of the infrared pump power on the emitter. The results show the superiority of the M3 and M4

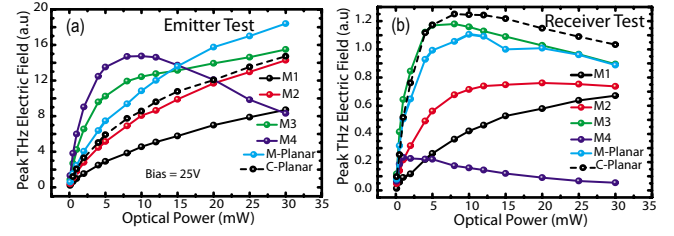


FIG. 3. (Color online) (a) Optical power dependence of the emitted THz radiation from each device. (b) Optical power dependence of the detected THz signal when devices were tested as receivers.

mesa multilayered devices under low optical excitation powers (up to 15 mW). For higher optical powers the performance of the planar multilayered device outperforms all the multilayered mesa devices as well as the planar conventional. It is interesting to note that the functional form of all devices, except for the M3 and M4 structures, show a monotonic increase with optical power in accordance with the scaling rule as follows:^{9,10} $E_{\text{THz}}^{\text{Peak}} = C[P/(P_0 + P)]$, where P is the optical power, C is a proportionality constant, and P_0 is a constant characterizing the saturation behavior of the device. The above equation describes the saturation of THz intensity as a result of THz radiation field screening of the bias field in large aperture photoconductive antennas, and is derived by applying the appropriate boundary conditions. Our previous work using a 2 μm gap photoconductive switches did not show any deviation from this scaling rule.¹¹ In this present work however, we observe in Fig. 3(a) that the M3 device shows a leveling off beyond 15 mW of optical power, and the M4 device shows a roll-off after reaching a peak at 7 mW of optical power. Although this rolling-off is usually not seen in conventional planar LT-GaAs photoconductive emitters, and is not explained by the scaling rule; its origin may be a consequence of the more complex boundary conditions in a 3D mesa type structure. Furthermore, defect saturation, which occurs at high optical powers, and/or lower emitter resistances, as observed in these mesa type devices, may also contribute to the rolling-off effect.¹¹

In the receiver configuration, again the performance is improved with increasing number of layers contacted (from M1 to M3). The M3 mesa defined photoconductive gap showed similar performance to the planar structure M-Planar, see Fig. 3(b). However, beyond 5 mW of optical power, the conventional planar device C-Planar, shows a slight enhancement in performance (to within 10%) over the M3 device. The final structure, M4, unexpectedly showed a very poor performance. This is a surprising result as it contradicts the expected reciprocity of the emitter-receiver performance due to the optical symmetry between the generation and detection processes.

In order to explain the above results and investigate the effect of the mesa geometry on device performance, a control experiment was performed. Here, mesa defined photoconductive gaps were fabricated on a conventional 1 μm LT-GaAs single layer. Figures 4(b) and 4(c) show the THz pulses collected from such devices having different mesa depths ranging between 500 nm to 1.2 μm , in the emitter and receiver configuration, respectively. The emitted and detected peak THz signal as a function of incident optical power is also shown in Figs. 5(a) and 5(b), respectively.

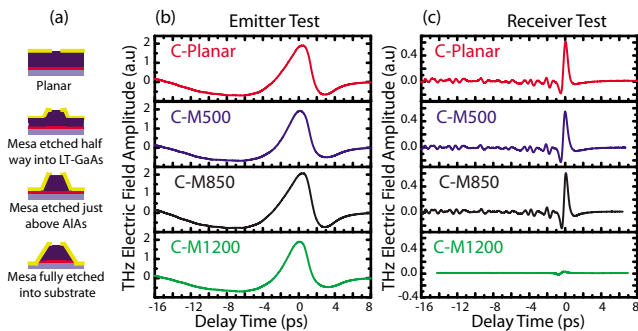


FIG. 4. (Color online) THz time domain signal from both, planar and mesa defined photoconductive switches fabricated on a standard $1\ \mu\text{m}$ thick LT-GaAs active region. Both (b) emitter and (c) receiver tests are shown. The measurements were taken at 5mW of optical power and a bias voltage of 50 V.

In the emitter configuration, the mesa structure had negligible effect on the device performance. Furthermore, the functional form of the saturation curves in Fig. 5(a) indicate a monotonic increase in accordance with the scaling rule. Hence, since no improvement in the THz emission was observed in the mesa defined photoconductive gaps using the single LT-GaAs layer structure, the results of Figs. 2 and 3 indicate that the multilayered nature of the device is solely responsible for the observed enhancement in THz emission. This is a significant result as it demonstrates the potential of achieving efficient and enhanced THz output power using complex LT-GaAs heterostructure device architectures, although in this case it was only demonstrated for low optical excitation. Furthermore, in another experiment,⁸ we have observed an identical THz performance from $1\ \mu\text{m}$, 500 nm, and 200 nm thick LT-GaAs planar photoconductive switches. This suggests that although photoelectrons are created deep in both the $1\ \mu\text{m}$ and 500 nm LT-GaAs layers, they are inefficient in the THz emission process. As Fig. 5(a) shows, the side contacts in the mesa devices did not improve the situation. However, in the multilayered structure, the inclusion of the AIAs isolation layers had a positive effect on the THz emission intensity. We believe this could be related to the inhomogeneous conduction inside a conventional planar LT-GaAs photoconductive switch, which leads to a poor coupling between the electron-hole hertzian dipole and the antenna structure. In the case of the multilayered devices, the AIAs layers sever to restrict the conduction in the plane of the antenna leading to better coupling to the electron-hole dipole, hence the observed enhancement.

Figures 4(c) and 5(b) show that in the case of a receiver, no significant degradation in the signal is observed until the

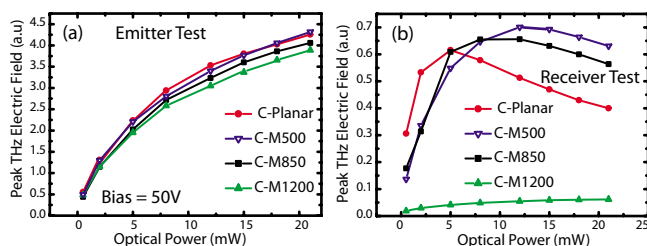


FIG. 5. (Color online) Optical power dependence of the (a) emitted and (b) detected THz radiation from planar and mesa defined photoconductive switches fabricated using a conventional $1\ \mu\text{m}$ thick LT-GaAs active region.

mesa etch depth reaches the SI-GaAs substrate, which is the case for device C-M1200. The deterioration in the receiver performance for devices having mesa etch depths reaching the SI-GaAs substrates is an indication that contact to the relatively conducting SI-GaAs substrate can significantly reduce the detection of the THz signal. This is a consequence of charge leakage through the SI-GaAs preventing accumulation of charge in the photoconductive switch capacitor. This conclusion is also supported by our recent study where it was found that charge accumulation in the photoconductive switch receiver, due to defect saturation, has an adverse effect on the receiver performance.¹¹ Interestingly, in the receiver configuration, all the mesa defined devices showed small improvements at high optical powers ($>5\ \text{mW}$) in comparison to the planar counterpart, in Fig. 5(b). In addition, we see a shift in the detected peak THz signal to high optical powers as the mesa depth increases.

Clearly, the poor performance of the multilayered mesa device, M4, can now be attributed to current leakage through the substrate which degraded its performance as a receiver. The enhanced THz detection with increasing layers in contact with the antenna electrodes could partially be due to the mesa geometry as shown in the case of single layered devices above, see Fig. 5. Such geometrical enhancement may be a result of the larger capacitance which can improve the THz detected signal.¹¹

In summary, we have fabricated a photoconductive switch with mesa defined photoconductive gaps on a multilayered LT-GaAs structure. The mesa geometry allowed contacts to be made through the different LT-GaAs layers, which resulted in commensurate improvements in the output THz power proportional to the number of LT-GaAs layers in contact with the antenna electrodes. Although the THz power enhancement was only observed for low optical excitation powers, the ability to achieve similar THz emission levels at lower excitation powers through this multilayered LT-GaAs mesa photoconductive switch could pave the way for producing arrays of photoconductive elements which can be excited using monolithically integrated waveguides. Furthermore, the mesa device geometry also facilitates edge coupling through such integrated waveguides, which could be achieved using low cost polymer waveguides such as PMMA.¹²

¹M. Tonouchi, *Nat. Photonics* **1**, 97 (2007).

²I. S. Gregory, C. M. Tey, A. G. Cullis, M. J. Evans, H. E. Beere, and I. Farrer, *Phys. Rev. B* **73**, 195201 (2006).

³S. M. Duffy, *IEEE Trans. Microwave Theory Tech.* **49**, 1032 (2001).

⁴J. E. Bjarnason, T. L. J. Chan, A. W. M. Lee, E. R. Brown, D. C. Driscoll, M. Hanson, A. C. Gossard, and R. E. Muller, *Appl. Phys. Lett.* **85**, 3983 (2004).

⁵R. Faulks, M. Evans, H. Page, S. Malik, I. Gregory, I. Farrer, D. Ritchie, and M. Pepper, *IEEE Photon. Technol. Lett.* **21**, 1603 (2009).

⁶E. A. Michael, B. Vowinkel, R. Schieder, M. Mikulics, M. Marso, and P. Kordos, *Appl. Phys. Lett.* **86**, 111120 (2005).

⁷M. Mikulics, E. A. Michael, R. Schieder, J. Stutzki, R. Güsten, M. Marso, A. van der Hart, H. P. Boehm, H. Lüth, and P. Kordos, *Appl. Phys. Lett.* **88**, 041118 (2006).

⁸S. Rihani, Ph.D. thesis, University of Cambridge, 2010.

⁹M. Tani, S. Matsuura, K. Sakai, and S. Nakashima, *Appl. Opt.* **36**, 7853 (1997).

¹⁰P. K. Benicewicz and A. J. Taylor, *Opt. Lett.* **18**, 1332 (1993).

¹¹S. Rihani, R. Faulks, H. Beere, H. Page, I. Gregory, M. Evans, D. A. Ritchie, and M. Pepper, *Appl. Phys. Lett.* **95**, 051106 (2009).

¹²H. Ma, A. Jen, and L. Dalton, *Adv. Mater. (Weinheim, Ger.)* **14**, 1339 (2002).